

THE DEPOSITION OF THIN METAL FILMS AT THE HIGH-INTENSITY PULSED-ION-BEAM INFLUENCE ON THE METALS

G.E.Remnev, A.N.Zakoutayev, I.I.Grushin, V.M.Matvienko, A.V.Potyomkin, V.A.Ryzhkov
Nuclear Physics Institute, Tomsk Polytechnic University, Tomsk, Russia

Yu.F.Ivanov
Construction Academy, Tomsk

E.V.Chernikov
Siberian Physical Technical Institute, Tomsk.

Abstract

The high-intensity pulsed ion beam with parameters: ion energy 350-500 keV, ion current density at a target $> 200 \text{ A/cm}^2$, pulse duration 60 ns) was used for the metallic deposition. Film deposition rate was 0.6-4.0 mm/s. Transmission electron microscopy/ transmission electron diffraction investigations of the copper target-film system have been performed. Impurity content in the film have been determined using X-ray fluorescence analysis and secondary ion mass spectrometry. The angular distributions of the ablated plasma have been measured.

Introduction

The high-intensity pulsed ion beam (HIPIB)/solid interaction results in the generation of an ablated plasma (10^{19} - 10^{20} cm^{-3} , 0.2-2 eV) which can be used to advantage for the deposition of thin films¹. The deposition process is analogous to pulsed laser deposition, but operates with higher total energy incident on a target allowing accelerated deposition rates or larger area coverage. The paper deals with the results of investigation on the deposition of metallic films, their structure and impurity content.

Experimental procedure

The basic experimental arrangement required for producing films by High-Intensity Pulsed-Ion Beam Deposition (HIPIBD) has been described in Ref. 6. Briefly, the study was carried out on TEMP-2 accelerator (ion energy 350-500 keV, ion current density at a target $> 200 \text{ A/cm}^2$, power density $(0.7$ - $1.5) \cdot 10^8 \text{ W/cm}^2$, pulse duration 60 ns, pulse repetition rate 8-10 min^{-1})².

Metallic deposition.

Transmission electron microscopy (TEM) and transmission electron diffraction (TED) investigations presented in Ref. 3, 4, 5, 6 showed that the metal films grown by the HIPIBD are polycrystalline formations containing both microparticles of the droplet fraction and microblisters (Fig.1a). The parameters (average sizes, linear density, volume fraction) of these structural formations depend on some conditions, including melting (evaporation) point, degree of cristallinity of a substrate, the quantity of pulses of the deposition, the number of depositing pulse, the diode-target-substrate geometry, as well as the structural and phase state of a target. Fig. 1b-g illustrates the results of analysis of the last factor influence. It has been

found that the influence of the high-intensity pulsed-ion beam (HIPIB) on the copper target is accompanied by changing the defect structure and phase composition of the metal.

(i) Carbon particulates with the cubic crystalline lattice ($a(\text{FCL})=0.421\text{nm}$) (Fig. 1 b-d) are observed on the target surface, with increasing the number of pulses of the HIPIB action the particulates' average sizes and their volume fraction increase. It was noted that on the target surface the particulates are the volume formations, frequently having a faceting, and in the near-surface layer ($\sim 0.5 \mu\text{m}$ layer thickness) the particulates are very thin disks (Fig. 1b).

(ii) Spherical particulates of the copper oxides are observed on the target surface. Their average sizes increase with increasing the number of pulses, but their linear density decrease. The near-surface layer has the gradiental defect structure: the nanocrystalline surface layer ($\bar{d}_{\text{cr}}=20 \text{ nm}$), the submicron near-surface layer ($\bar{d}_{\text{cr}}=300 \text{ nm}$, Fig. 1e,f). Crystallite sizes of this layer increase with increasing the number of pulses of the HIPIB action. The HIPIB influence on the metal is accompanied by changing the relief of the sample polished face (Fig. 1 f, g). It has been found that both a wave length and a degree of the relief periodicity depend on the number of pulses of HIPIB, metals, as well as the state of a metal that can be either a polycrystal (Fig. 1g) or a monocrystal (Fig. 1h).

Impurity content measurements in films.

The super-high rate of the film deposition by HIPIBD allows to produce films with the low impurity content, especially with impurities of light gaseous elements, such as C, N, O, constantly being in residual atmosphere ($P=5 \cdot 10^{-5}$ Torr). We have carried out a number of experiments dealing with the sputtering of high-purity (999.9) W and Au targets. The initial high-purity targets were certificated by the charged particle activation analysis (CPAA) method⁷. The films were deposited on high-purity AsGa plates with the content of C, N and O less 10^{-5} %. A thickness of the deposited films was determined by X-ray fluorescence analysis method with the excitation by photon radiation ^{109}Cd and the registration of the characteristic X-ray radiation of elements by Si(Li)-detector. For instrumental CPAA determination of C and N both in the films and on the AsGa substrates surface we used the irradiation by deuterons of a cyclotron with the energy of $\sim 3.1 \text{ MeV}$ in He-atmosphere and subsequence determination of induced activity of analytical radionuclides ^{13}N and ^{15}O with periods of half-decay 9.965 min and 2.04 min, respectively. The table presents the total content (surface density q) and the relative content (f_{θ}) of C and N in the W films, a background (surface contents in AsGa substrates: $q_{\text{C}}(\text{AsGa})=0.8 \mu\text{g}/\text{cm}^2$ and $q_{\text{N}}(\text{AsGa})=0.3 \mu\text{g}/\text{cm}^2$) being taken into consideration. The content of C and N in gold films was lower than a limit of determination $q_{\text{min}} \approx 0.3 q_{\text{C}}(\text{AsGa}) \approx 0.3 q_{\text{N}}(\text{AsGa})$. Quantitative estimates of the film impurity content were made using the secondary ion mass spectrometry also.

Table. Impurity contents of C and N in the W films.

The number of pulses	$q_{\text{W}}, \mu\text{g}/\text{cm}^2$	$q_{\text{C}}, \mu\text{g}/\text{cm}^2$	$f_{\text{C}}, \text{wt. \%}$	$q_{\text{N}}, \mu\text{g}/\text{cm}^2$	$f_{\text{N}}, \text{wt. \%}$
30*	0.45	2.3	0.51	0.77	0.17
100**	1.1	11.8	1.1	0.97	0.09
100***	1.3	9.7	0.75	0.62	0.05

- without preliminary sputtering of the target surface and without nitrogenous trop;
- with preliminary sputtering of the target surface and without nitrogenous trop;
- with preliminary sputtering of the target surface and with nitrogenous trop.

The performed investigation allows to conclude the following:

- (i) The content of C in the W films is an order of magnitude higher than the content of N, but the C total quantity is proportional to the number of pulses, that indicates the contamination of the films by gases of residual atmosphere of the work chamber during the deposition process.
- (ii) The preliminary sputtering of the W target surface decreases a level of the N contamination of the produced films by two or three times and doesn't influence a level of the contamination caused by the C-containing compounds that determining a degree of vacuum in the work chamber.
- (iii) The lack of detectable quantities of C and N in gold films indicates the chemical nature of the gas contamination in the W films.
- (iv) The contamination of the films occurs during breaks between pulses after the deposition of the ablated plasma plume onto a substrate.

Thus, we have presented a possibility to produce high-purity films of noble metals (Au, Ag, platinumoids) from the ablated plasma at sputtering initial high-purity targets by HIPIB. Pure films of chemically active metals may be produced if to improve a vacuum in the work chamber.

The angular distribution of the ablated plasma.

The HIPIB with the following parameters: 350 keV ion energy, 250 A/cm² current density at a target, 8.75 · 10⁷ W/cm² power density at target, 60 ns pulse duration, 5.25 J/cm² fluence at target, was used in the experiments. A diagram of the experimental system for angular measurements is shown schematically in Fig. 2a. All the targets were tablet-shaped with S=1 cm². Energy-disperse X-ray fluorescence analysis via X-ray excitation of ¹⁰⁹Cd and measuring of characteristic X-rays of elements by Si(Li)-detector was used for determination of surface density of ZnS, Nb, W, Au, Pb films with a thickness of 0.2-400 nm for studying the angular distributions of the sputtered products. Standard relative deviation of the XRF results was 0.01-0.3 for the thickest and thinnest layers of the sputtered products, respectively. To measure an angular distribution of C (graphite), Al, Si and Al₂O₃ (leucosapphire) the autoradiography technique based on the 3 MeV-deuteron activation is developing now. The plume of the ablated plasma is cone-shaped and characterized by a highly forward peaked distribution, $\exp(-n|\theta|)$ with 3 < n < 4.5, where θ is measured with respect to the target normal (Fig. 2a, b). This is in contrast to what one expects from a purely thermal evaporation characterized by a $\cos(\theta)$ distribution.

Conclusion

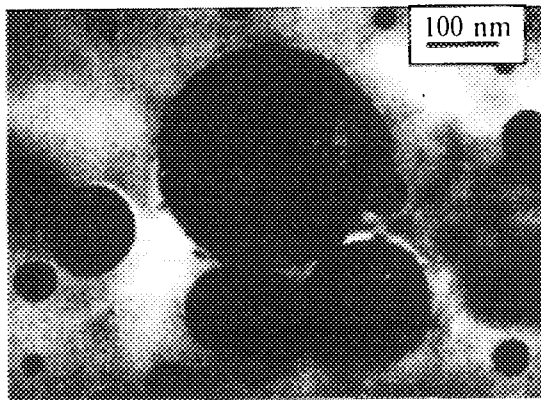
The joint, TEM/TED investigations of the copper target-film system have been performed. The modifying influence of HIPIB on the structure and phase composition of the target has been determined, a connection between the structure of the target and that of the film being revealed. The angular distribution has an exponential behavior, and the exponential parameter for investigated materials is ranged from 3 to 4.5 depending on the sort of materials. The influence of pressure of residual atmosphere to concentration of elements, which form gases, is investigated.

Acknowledgment

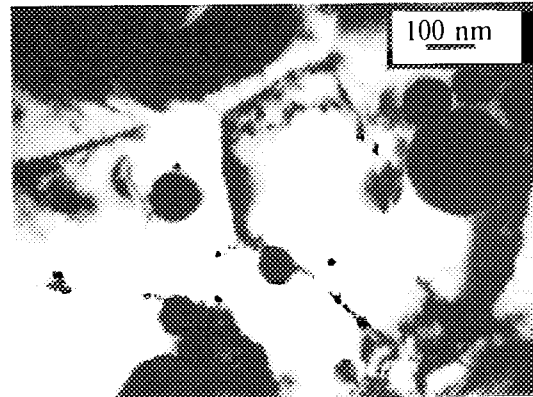
This work is supported by the contract 1631 Q0014-35 between University of California, Los Alamos National Laboratory and Tomsk Nuclear Physics Institute for Materials Processing with Intense Ion Beams.

References

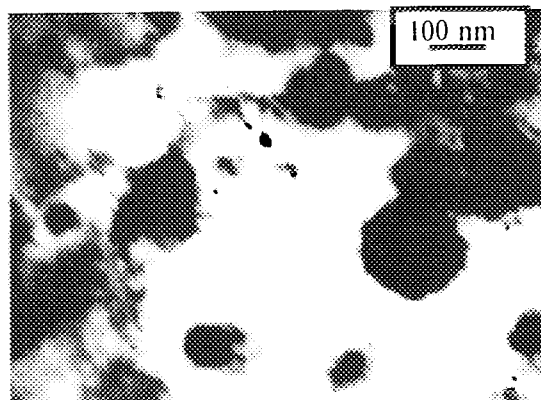
- ¹ H. A. Davis, G. E. Remnev, R. W. Stinnet and K. Yatsui, *MRS Bulletin*, 1996 (in press).
- ² G. E. Remnev, I. F. Isakov, G. E. Kotlyarevsky et al., in *Proc. of 9th Intern. Conf. on Surface Modification of Metals by Ion Beams*, San Sebastian, Spain, 1995 (to be published).
- ³ A. N. Zakoutayev, G. E. Remnev, Yu. F. Ivanov, M. S. Artyev, V. M. Matvienko, and A. V. Potyomkin, in *Film Synthesis and Growth Using Energetic Beams*, edited by H. A. Atwater, J. T. Dickinson, D. H. Lowndess, and A. Polman (Mater. Res. Soc. Proc. **388**, Pittsburgh, PA, 1995), pp. 388-393.
- ⁴ Yu. F. Ivanov, G. E. Remnev, A. N. Zakoutayev, V. M. Matvienko, A. V. Potyomkin, in *Proc. of IV Conf. on Modification of Structural Materials by Charged Particle Beams*, Tomsk, 1996, pp. 442-444.
- ⁵ Yu. F. Ivanov, G. E. Remnev, A. N. Zakoutayev, V. M. Matvienko, A. V. Potyomkin, submitted to *Sov. Tech. Phys. Letters* (1996).
- ⁶ Yu. F. Ivanov, V. M. Matvienko, A. V. Potyomkin, G. E. Remnev, A. N. Zakoutayev, in *Ion-Solid Interactions for Materials Modification and Processing*, edited by D. B. Poker, D. Ila, Y-S. Cheng, L. R. Harriott, and T. W. Sigmon (Mater. Res. Soc. Proc. **396**, Pittsburgh, PA, 1996)
- ⁷ Ryzhkov V. A., Oblivantsev A. N., Rybasov A. G., *High-purity substances* (Russia), 1995, No. **6**, pp. 49-53.



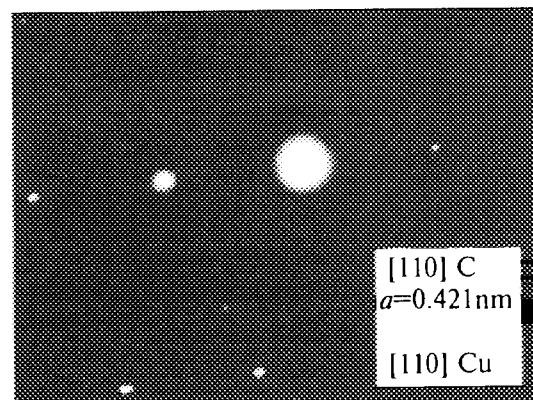
(a)



(b)



(c)



(d)

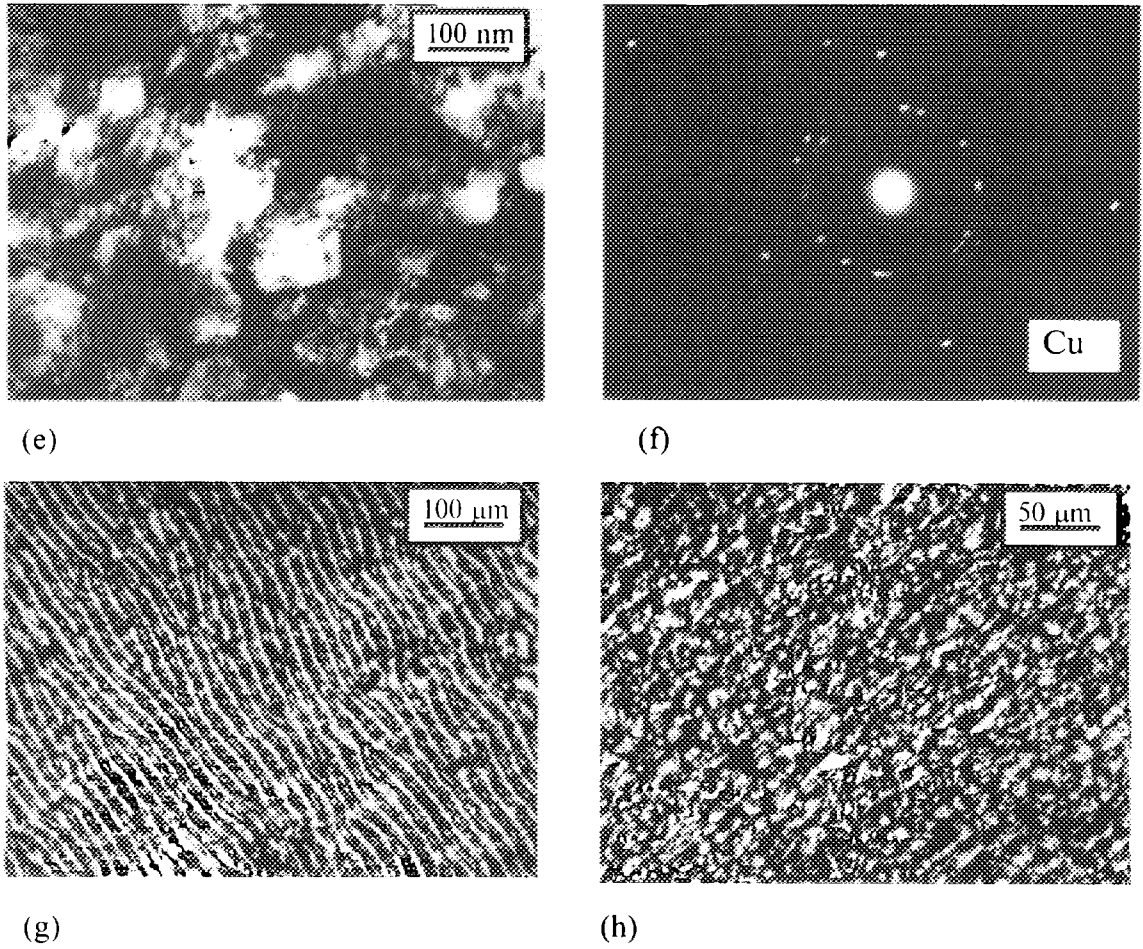


Fig. 1, (a, b, c, e) TEM, (d, f) TED and (g, h) optical images of the structure of both (a) the Cu film and (b, d) the Cu target obtained at sputtering both (a-f) a polycrystal and (g) a monocrystal.

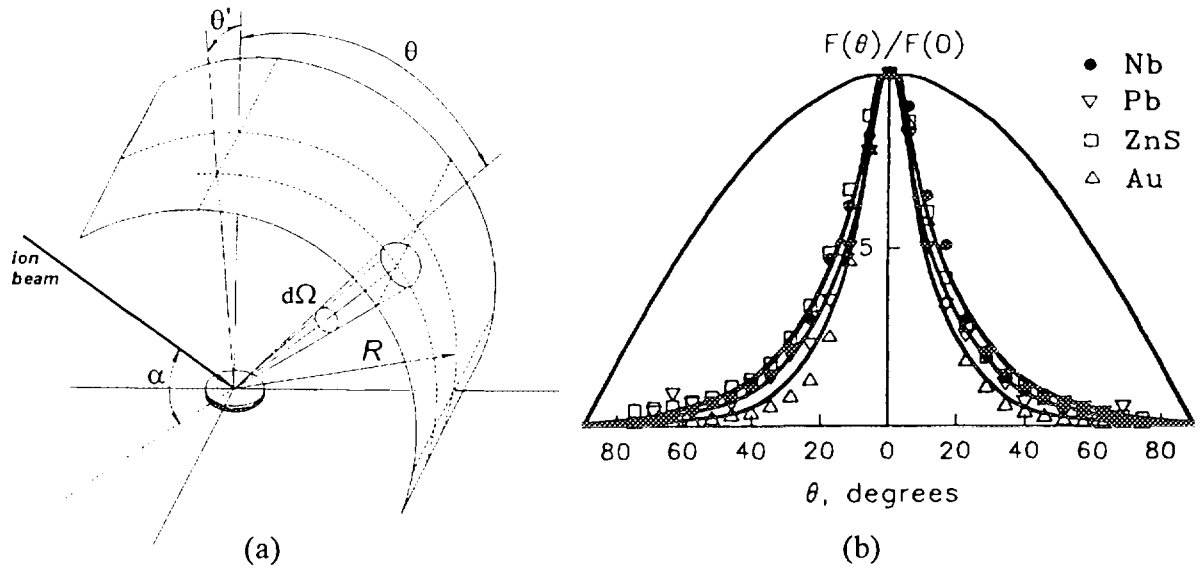


Fig. 2, (a) Schematic diagram of the angular measurements; (b) Angular distributions of the ablated plasma (Nb $\sim \exp(-3.1|\theta|)$, Pb $\sim \exp(-3.4|\theta|)$, ZnS $\sim \exp(-3.0|\theta|)$, Au $\sim \exp(-4.3|\theta|)$, a $\cos(\theta)$ distribution is presented for comparison).